

# Phase locked second and third harmonic localization in semiconductor cavities

V. ROPPO<sup>a,b</sup>, C. COJOCARU<sup>a</sup>, G. D'AGUANNO<sup>b</sup>, F. RAINERI<sup>c,d</sup>, J. TRULL<sup>a</sup>, Y. HALIOUA<sup>c,e</sup>, R. VILASECA<sup>a</sup>, R. RAJ<sup>c</sup>, M. SCALORA<sup>b</sup>

<sup>a</sup>Universitat Politècnica de Catalunya, Dept. de Física i Eng. Nuclear, Colom 11, 08222 Terrassa, SPAIN

<sup>b</sup>C. M. Bowden Research Facility, US Army, RDECOM, Redstone Arsenal, AL 35803, USA

<sup>c</sup>Laboratoire de Photonique et de Nanostructures (CNRS), Marcoussis, FRANCE

<sup>d</sup>Université Paris-Diderot, 75205 Paris Cedex 13, FRANCE

<sup>e</sup>Ghent University-IMEC, Depart. of Information Technology- Sint-Pietersnieuwstraat 41, 9000 Gent, BELGIUM

---

We study the enhancement of the second and third harmonic generation using ultra short pulses in a cavity environment, focusing on the role of the phase locking phenomena. Despite the fact that the cavity is only resonant at the fundamental frequency and the harmonics are tuned in a spectral range of huge nominal absorption, we predict and experimentally observe the harmonics become localized inside the cavity leading to relatively large conversion efficiencies. This unique behavior reveals new optical phenomena and new applications for opaque nonlinear materials (i.e. semiconductors) in the visible and UV ranges.

(Received December 15, 2009; accepted January 20, 2010)

*Keywords:* Nonlinear optics, Harmonics generation, Semiconductor

---

## 1. Introduction

The study of harmonics generation begins in the early 1960s with the theoretical and experimental works on second harmonic (SH) generation [1, 2]. By now second harmonic generation (SHG) is a well-understood phenomenon that finds practical applications in many areas. Second and higher harmonics arise thanks to the nonlinear relation that links the polarization to the electromagnetic fields. In most cases this relation can be assumed to behave linearly. However, when the intensity of the incident pump field or fields is high enough and/or if the nonlinear coefficients of the material are relatively high, nonlinear effects may become important. To date, most researchers' efforts have been directed at improving the efficiency of the harmonic generation process by engineering new materials with higher effective nonlinear coefficients, accompanied by phase and group velocity matching [3-6]. This is why most studies have been concerned with maximizing conversion efficiencies through the achievement of phase matching (PM) conditions, i.e. an attempt at equalizing the relative phases of the beams to ensure maximum energy transfer from the fundamental (FF) beam to the second or third harmonic (TH) signals. Outside of PM condition the efficiency decreases rapidly [7]. The resulting low conversion efficiency is the reason why propagation phenomena in the mismatched regime remain largely unexplored.

## 2. Phase locked harmonic localization

Recently, an effort was initiated to more systematically study the dynamics of second and third harmonic generation in transparent and opaque materials under conditions of phase mismatch [8-11]. The dynamic of the phase locking (PL) mechanism is deeply related with the harmonic generation theory. As outlined in the seminal work [2], the energy transfer between the fundamental field and its generated SH always happens at the interface and it is limited near it. Then, how much near depends on the working conditions and the dimensions of the pulses and samples. Generally speaking, the SH pulse will always experience an index of refraction bigger than the fundamental and thus will travel slower. The exchange of energy will take place from the interface up to when the walk-off of the two pulses is complete and the harmonic pulse is not longer under the influence of the fundamental pulse due the velocity difference.

With these considerations in mind, it not surprising to bury the fact that when a fundamental (pump) pulse crosses an interface between a linear and a nonlinear medium there are always *three* generated SH and/or TH components. One component is generated backward into the incident medium, due the index mismatch between the materials that form the interface and the other two are generated forward. The basis for understanding the generation of two distinct forward-moving signals is based on the mathematical solution of the homogeneous and inhomogeneous wave equations at the SH frequency [2]. Continuity of the tangential components of all the fields at the boundary leads to generation of the two forward-

propagating components that interfere in the vicinity of the entry surface and give rise to Maker fringes [12]. It turns out that while the inhomogeneous component is captured by the pump pulse and experiences the same effective dispersion of the pump [8-11], the homogeneous component travels with the group velocity given by material dispersion. That is, this component has wave-vector  $k_{2\omega}^{HOM} = n(2\omega)k(2\omega)$  (where  $k(2\omega)$  represents the free space wavevector at the frequency  $\omega$ ) and exchanges energy with the pump until the inevitable walk-off. On the other hand, the inhomogeneous (phase-locked) component has a wave-vector given by  $k_{2\omega}^{PL} = 2n(\omega)k(\omega)$ , twice the pump's wave-vector. Analogue situation is found for the TH.

In ref. [10] it was shown theoretically that the real part of the effective index of refraction that the harmonics experience is equal to that of the pump. This may be done by performing a full spectral decomposition of the fields, and by calculating the effective index of refraction  $n_{\text{eff}} = \langle k \rangle / \langle \omega \rangle$  as the ratio of expectation values

$$\langle k \rangle = \int_{k=-\infty}^{k=\infty} k |H(\omega, k)|^2 dk \quad \text{and} \quad \langle \omega \rangle = \int_{\omega=-\infty}^{\omega=\infty} \omega |H(\omega, z)|^2 d\omega.$$

The E field may also be used in the calculation. Once the real part of the index  $n_{\text{eff}}$  is mapped onto the pump index of refraction, the imaginary part of the index is obtained by performing a Kramers-Kronig reconstruction, which in turn yields an imaginary part for the second harmonic field that is identical to the index of refraction for the pump field. Experimental evidences of such behaviour are given in refs. [10] and [13].

It is important to point out that the two harmonics components have different nature and respond differently to the surrounding environment. The inhomogeneous component travels in phase with the pump and once its energy is settled does not exchange any more energy with it (phase locked). Every nonlinear interface (namely, jump of the value of the nonlinearity) or perturbation in the linear and/or nonlinear characteristics of the material provokes a disengagement or a generation of a new inhomogeneous component. On the other hand, the behaviour of the homogeneous component is well known, and relies only on the dispersion properties at its frequency. Even because the usual working conditions tend to approach the phase matching, when this last component is present it is generally bigger than the phase locked one causing its observation difficult. This can be the reason why it needed more than 40 years to start a systematic study on this topic [8].

It is straightforward now to think the possibility to completely separate the destinies of the two components, letting them to propagate in a situation where there is a substantial difference between the fundamental and second and/or third harmonic indexes of refraction. In the ref. [10], the nonlinear material is chosen to be GaAs. The pump at 1300nm is tuned in the transparent region and the SH and TH (650nm and 433nm, respectively) are well deep into the absorption region. In this situation the homogeneous component is completely absorbed after

hundreds of nanometres and the only observable SH is the phase locked component. The study of the behaviour of the PL component can be far reaching because they open the door to new scenarios by allowing working conditions hitherto assumed inaccessible for absorbing materials, semiconductors in particular.

Even if the use of the GaAs is not mandatory for the purpose of this work, we chose to work with in the same situation of ref. [10]. In this way it is possible to isolate and focus all the attention on the PL component. The aim is to explore its behavior in a cavity environment. If the PL component reads the same index of refraction of the fundamental pulse, how does it behave in a cavity designed to be resonant at the fundamental frequency? The answer is that the PL mechanism not only inhibits absorption, but also fosters the enhancement of harmonic generation by several orders of magnitude compared to the no-cavity case due to the double action of fundamental field localization and *anomalous harmonic field localization*. While the role of the first one is easily understandable, an explanation is needed to clarify the role of the harmonic field localization.

The dispersion curves for GaAs, shown in Fig.1, shows that this material is transparent at wavelengths above 900nm, and completely opaque below 900nm. Now let us consider the optical thickness of the GaAs layer around two wavelengths length inside the material, so that the pump field resonates. The complex refractive index of GaAs is  $n(1300\text{nm})=3.41$ ,  $n(650\text{nm})=3.83+i0.18$  and  $n(433\text{nm})=5.10+i1.35$ , as reported by Palik [14]. Conventional wisdom dictates that this structure should be resonant for the fundamental, but not for the SH and TH signals due to the optical thickness and material absorption. While this is true for the homogeneous components, the PL mechanism causes the inhomogeneous components to resonate inside the cavity along with the pump. So, the inhibition of absorption demonstrated in ref. [10] is accompanied by a pull of the harmonics, initially tuned far from any cavity resonance, into an effective resonant condition. The phenomenon will occur with any nonlinear absorbing material, including negative index material and semiconductors in the metallic range [15].

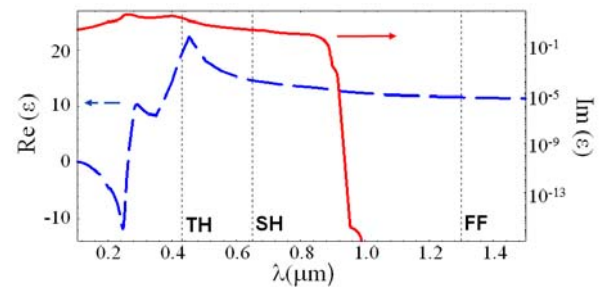


Fig.1. Absorption spectra of GaAs as in ref.[11]. The tuning of the fundamental and its SH and TH are marked.

#### 4. Design and optimization of the cavity

To put into evidence the role played by the PL mechanism in a cavity configuration we have performed a numerical study aimed at finding the best possible experimental conditions. We have considered two basic designs: a standard cavity in GaAs with gold mirrors on both ends of the sample for simultaneous forward and backward SHG, and a second cavity with only one back mirror for backward SHG. These two configurations are shown in Fig.2.

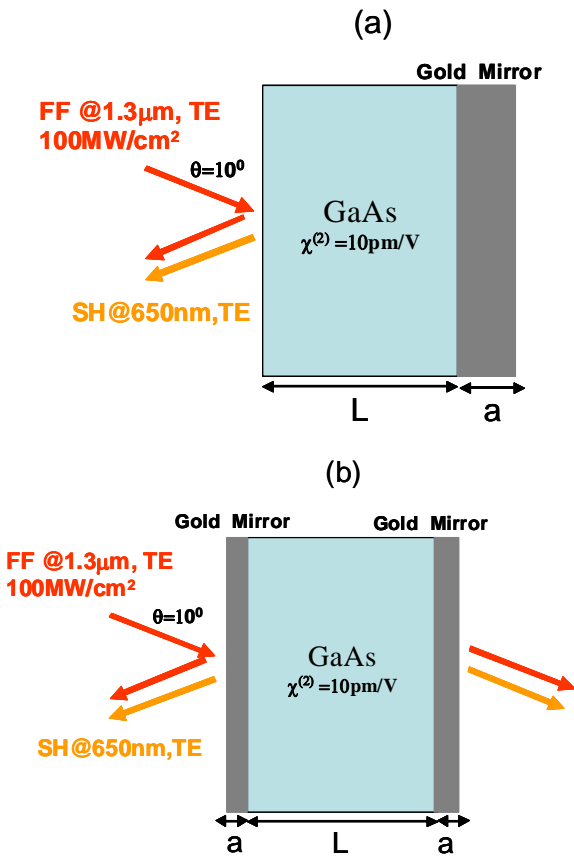


Fig.2. Schematic representation of the two considered geometries.

The SHG calculations have been performed using a Green function approach as detailed in Ref. [16]. The length of the GaAs and the thickness of the mirrors have been varied simultaneously for both configurations and the corresponding SHG calculated. The refractive index and extinction coefficient for GaAs and Au are taken from experimental measured data [14]. The results for the configuration (a) are shown in Fig.3, while the results for the configuration (b) are shown in Fig.4. In Fig.3 we note that for the configuration (a) the best SH conversion efficiency, of the order of  $10^{-8}$ , is obtained for a length of the GaAs of  $\sim 645\text{nm}$  and a length of the back mirror equal or greater than  $80\text{nm}$ . This maximum conversion

efficiency has been obtained considering an input intensity of  $\sim 100\text{MW}/\text{cm}^2$  and an estimated value of  $\sim 10\text{pm}/\text{V}$  for the GaAs nonlinearity at an incident angle of  $\sim 10^\circ$ .

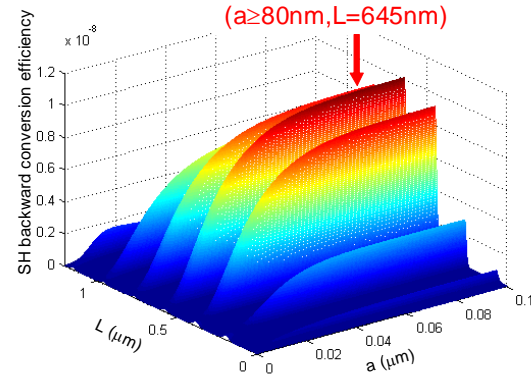


Fig.3. SH conversion efficiency vs. length of the GaAs and thickness of the back mirror for configuration (a) in Fig.2.

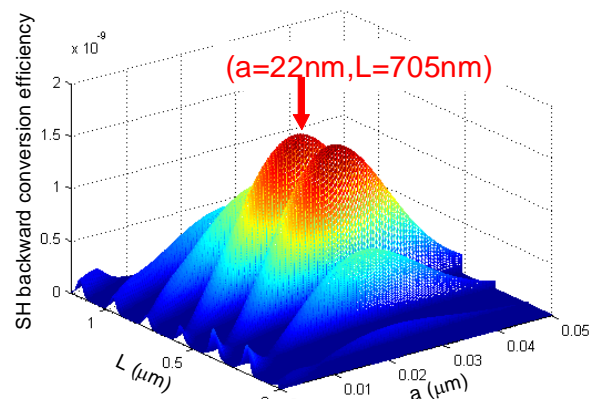
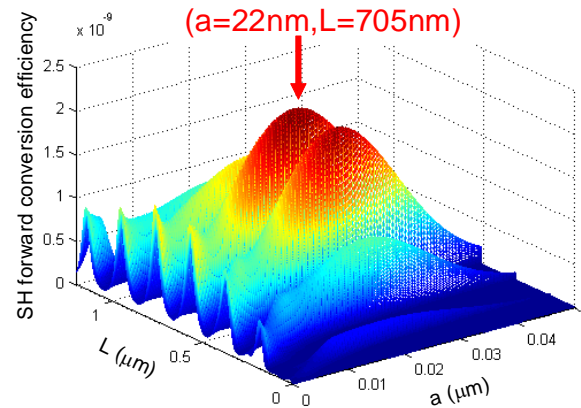


Fig.4. SH conversion efficiency vs. length of the GaAs and thickness of the mirrors for configuration (b) in Fig 2.

On the contrary, in Fig. 4 we note that the configuration (b) is far less efficient than the configuration (a), in fact we get a total (forward+backward) conversion efficiency of  $\sim 3.5 \cdot 10^{-9}$  which should be contrasted with a backward conversion efficiency of  $\sim 10^{-8}$  for the configuration (a). In Fig. 5 we compare the spectral bandwidth of the SH emission as function of the incident wavelength. From Fig. 3 it is evident that configuration (a) not only ensures a greater SHG, but also a better tunability.

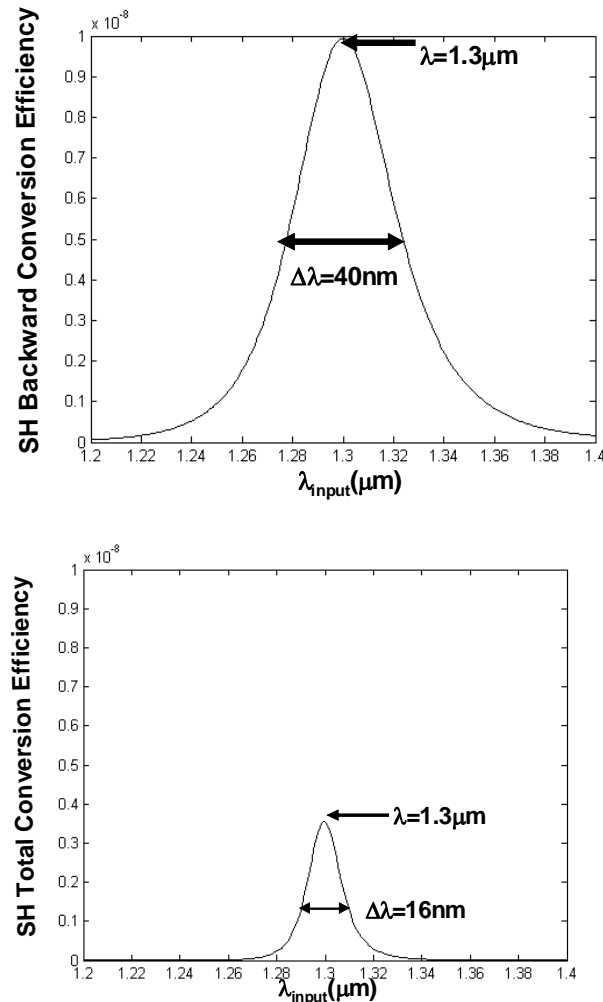


Fig. 5. Spectral bandwidth of the SHG for configuration (a) and (b).

Finally, before closing this section, we would like to spend few words about the crucial role played by the back mirror in the enhancement of the SH emission in the configuration (a). In Fig. 6 we show the SH emission with and without the back mirror. The SHG with the back mirror is  $\sim 35$  times greater than the SHG with no back mirror.

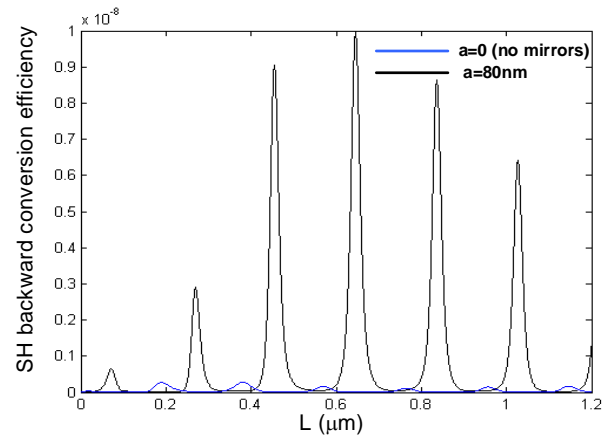


Fig. 6. SHG from a simple GaAs etalon (no mirror) and from the same GaAs etalon plus a back mirror of 80 nm.

## 5. Experimental results and discussions

In Fig. 7 is shown in detail the fabricated sample scheme (Fig. 7a) and the experimental set-up (Fig. 7c). Linear reflectivity of the used cavity was taken by Fourier Transform Infrared Spectroscopy (FTIR). This reflectivity and a comparison with the predicted one are shown in Fig. 7b. The linear reflectivity clearly shows a resonance at the fundamental wavelength (1300 nm) and no resonance at the SH wavelength (650 nm).

In our experiment we used a typical reflection measurement set-up. The source consists of 120 fs pulses from an OPA laser working at 1 KHz repetition rate, with tunable wavelength between 1200 and 1600 nm. The beam power was of 200 MW and was focused on the sample down to a  $\sim 0.5$  millimeter spot size, with corresponding peak intensity of  $\sim 5$  GW/cm<sup>2</sup>. The reflected signal was collected and analyzed with a spectrometer connected to a cooled Si CCD camera. Due to the nonlinearity of the material, a second and third harmonics fields will be generated and recorded.

Nine different measurements were performed from 1260 nm up to 1420 nm in 20 nm wavelength steps (Fig. 8). As references, the SH and TH signals generated from a simple Au mirror and a bulk GaAs sample, as well as the background illumination, were recorded with the same set-up and subtracted from the harmonic signals recorded with our sample. These references show clearly that surface SH and TH signals generated by the bulk GaAs and gold samples are negligible with respect to the harmonics generated by the cavity. Two generation peaks are clearly visible at 650 and 433 nm, indicating that while the fundamental is scanning the resonance at 1300 nm the SH and TH are resonating as well. In Fig. 9 is reported the calculated and measured reflection spectra. The bandwidths of these signals are in good agreement with the ones forecast with the CW approach (Fig. 8 dashed line).

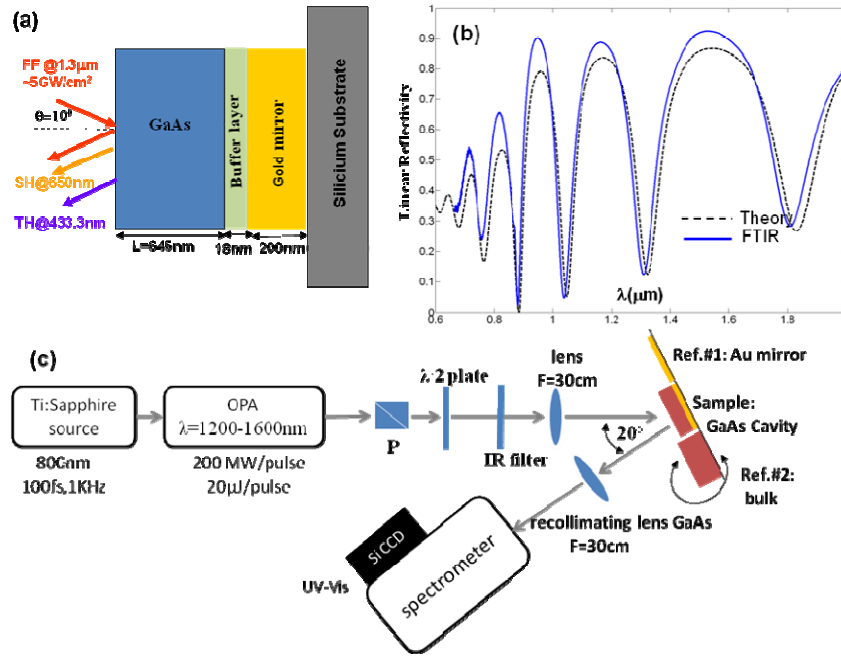


Fig. 7. (a) Sample's scheme; (b) Linear reflectivity of the sample taken by Fourier Transform Infrared Spectroscopy (FTIR) and comparison with theory. (c) Experimental set-up.

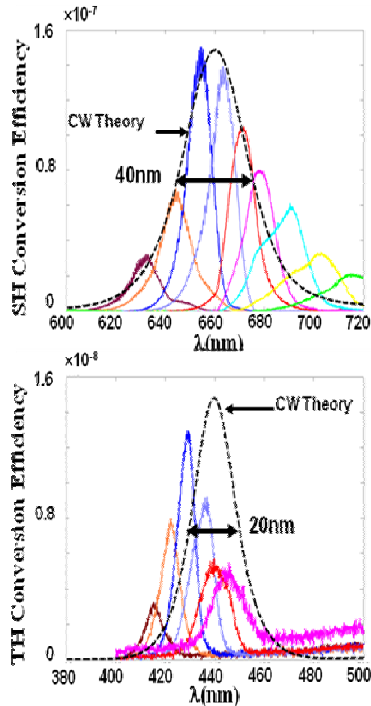


Fig. 8. Experimental results for SH (c) and TH (d) signals. The dashed black curves represent the CW theory. The different curves represent the harmonic signals for different pump tunings (respectively from left to right 1260nm, 1280nm, 1300nm, 1320nm, 1340nm, 1360nm, 1380nm, 1400nm, 1420nm). We note that the bandwidths of the signals are in excellent agreement with the numerical predictions.

## 6. Conclusion

Starting from the experience in ref. [10] we outlined the general behavior of the generated harmonics from a nonlinear material interface. Always present is the phase locked component with the peculiar characteristic, once generated, to not exchange energy with the FF field during the bulk propagation. Its energy is fixed and generally orders of magnitude lower than the homogeneous component. This is because the usual working conditions tend to approach the phase matching situation where a net flux of energy is spilled from the FF to the homogeneous component causing the observation of the PL component difficult. We can maybe find here the reason why it needed more than 40 years to start a systematic study on this topic [8].

In the second part of this work the phase locking phenomenon has been fully investigated in a cavity environment revealing the possibility to enhance the harmonics conversion efficiency thanks to the synergistic action of the fields' localization.

Finally, the theory has a generality wide enough to covers, for our knowledge, every situation where a harmonic field is generated. Thanks to the cavity environment a new range of possible applications can be thought able to take the most of the phase locking effect as, for example, frequency laser conversion towards the UV and XUV ranges.

## Acknowledgments

We thank the U.S. Army European Research office for partial financial (support project W911NF). G.D.

thanks the National Research Council for financial support. V.R., C.C., J.T. and R.V. acknowledge support from the Spanish government through Project No. FIS2008-06024-C03-02/FIS. We also thank Nadia Mattiucci and Mark J. Bloemer for helpful discussions and suggestions.

## References

- [1] P. A. Franken, A. E. Hill, C. W. Peters, G. Weinreich, *Phys. Rev. Lett.* **7**, 118 (1961).
- [2] N. Bloembergen, P. S. Pershan, *Phys. Rev.* **128**, 606 (1962).
- [3] J. T. Manassah, O. R. Cockings, *Opt. Lett.* **12**, 1005 (1987).
- [4] L. D. Noordam, H. J. Bakker, M. P. de Boer, H. B. van Linden van den Heuvell, *Opt. Lett.* **15**, 1464 (1990).
- [5] R. M. Rassoul, A. Ivanov, E. Freysz, A. Ducasse, F. Hache, *Opt. Lett.* **22**, 268 (1997).
- [6] W. Su, L. Qian, H. Luo, X. Fu, H. Zhu, T. Wang, K. Beckwitt, Y. Chen, F. Wiseet al., *J. Opt. Soc. Am. B* **23**, 51 (2006).
- [7] J. A. Armstrong, N. Bloembergen, J. Ducuing, P. S. Pershan, *Phys. Rev.* **127**, 1918 (1962).
- [8] V. Roppo, M. Centini, C. Sibilìa, M. Bertolotti, D. de Ceglia, M. Scalora, N. Akozbek, M. J. Bloemer, J. W. Haus, O. G. Kosareva, V. P. Kandidov, *Phys. Rev. A* **76**, 033829 (2007).
- [9] V. Roppo, M. Centini, D. de Ceglia, M.A. Vicenti, J. H. Haus, N. Akozbek, M. J. Bloemer, M. Scalora, *Metamaterials* **2**, 135 (2008).
- [10] M. Centini, V. Roppo, E. Fazio, F. Pettazzi, C. Sibilìa, J.W. Haus, J. V. Foreman, N. Akozbek, M. J. Bloemer, M. Scalora, *Phys. Rev. Lett.* **101**, 113905 (2008).
- [11] V. Roppo, C. Cojocaru, F. Raineri, G. D'Aguaño, J. Trull, Y. Halioua, R. Raj, I. Sagnes, R. Vilaseca, M. Scalora, *Phys. Rev. A* **80**, 043834 (2009).
- [12] P. D. Maker, R. W. Terhune, M. Nisenoff, C. M. Savage, *Phys. Rev. Lett.* **8**, 21 (1962).
- [13] E. Fazio, F. Pettazzi, M. Centini, M. Chauvet, A. Belardini, M. Alonzo, C. Sibilìa, M. Bertolotti, M. Scalora, *Opt. Express* **17**, 3141 (2009).
- [14] E. D. Palik ed., *Handbook of Optical Constants of Solids* (Academic, New York, 1985).
- [15] N. Akozbek, V. Roppo, M. A. Vincenti, J. V. Foreman, M. J. Bloemer, J.W. Haus, M. Scalora, <http://arxiv.org/abs/0904.4082>.
- [16] N. Mattiucci, G. D'Aguaño, M. Scalora, M. J. Bloemer, *Phys. Rev. E* **72**, 066612 (2005).

---

\*Corresponding autor: Vito Roppo (vito.roppo@upc.edu)